JOURNAL OF MATERIALS SCIENCE 10 (1975) 1841–1848

An esr study of electron and hole trapping in gamma-irradiated Pyrex

G. BROWN
Physics Department, Royal Military College of Science, Shrivenham, Swindon, Wiltshire, UK

Electron and hole resonances, produced by γ-irradiation of Pyrex, are investigated by electron spin resonance (esr) at X-band. It is proposed that the electron traps which generate the narrow g = 2.0008 resonance arise, not from the bulk borosilicate structure, but from a sub-microscopic silica glass structure. Growth curves of the trapped electron and hole populations show a two-stage behaviour with increasing dose. In order to explain the growth characteristics in the low-dose region, a non-paramagnetic trapped-electron population is postulated.

1. Introduction

The first observations of electron spin resonance (esr) in γ-irradiated glasses were made by Yasaitis and Smaller [1]. Since then, the esr study of γ-induced defect centres in glasses has proved to be a most powerful tool for probing glass structure. Work in this field has been complemented by studies on paramagnetically-doped glass, and each method has yielded valuable insight into the environments which exist in various types of glass.

A recent study [2] has revealed a two-stage behaviour in the γ-dose dependence of the Fe^{3+} concentration in commercial Pyrex. The present paper continues the exposition of these results, showing that all the trapping processes undergo marked changes as the dose increases. Evidence is presented of a silica substructure in borosilicate and bisilicate glasses, together with less direct evidence of a non-paramagnetic cluster-type of electron trap.

2. Experimental

Commercially-available Pyrex tubes, 4 mm outer diameter and 1 mm wall thickness, were used as samples for the experiments. The tubes were γ-irradiated by a ^{60}Co source at a dose rate of about 1.5 Mrad h^{-1}. (The rad is a commonly used unit of energy absorption. An absorbed dose of 1 Mrad corresponds to an energy absorption input of 10 J.) The esr spectra were recorded at X-band on a JEOL spectrometer type PE-1X. First-derivative spectra were recorded in the usual way, with a modulation frequency of 100 kHz. Second-derivative spectra were obtained using simultaneous modulation at 100 kHz and 80 Hz, followed by sequential phase-sensitive demodulation. The microwave power is given in the text where necessary, and refers to the power incident on the cylindrical H_{011} cavity. Spin calibrations were performed using a standard $CuSO_4 \cdot 5H_2O$ single crystal attached to the Pyrex tube being examined. All experiments were carried out at room temperature.

3. Results

3.1. The trapped-electron signal

Gamma-irradiated Pyrex exhibits the well-known boron–oxygen hole centre (BOHC) signal, first studied by Lee and Bray [3] and subsequently by Griscom *et al.* [4] and by Taylor and Griscom [5]. At high microwave powers (about 40 mW), only the "five-line-plus-a-shoulder" spectrum is evident but, on reducing the power below about 0.5 mW, a narrow component becomes visible at g = 2.0008 (referred to g = 2.0036 for DPPH). Fig. 1 illustrates the two spectra. The narrow component first becomes visible at a dose of 2.5 Mrad and is easily saturated by the microwave power, indicating that the spin-lattice relaxation time is quite long. The complete power saturation shown in Fig. 1 can be put to good use in the evaluation of the number of

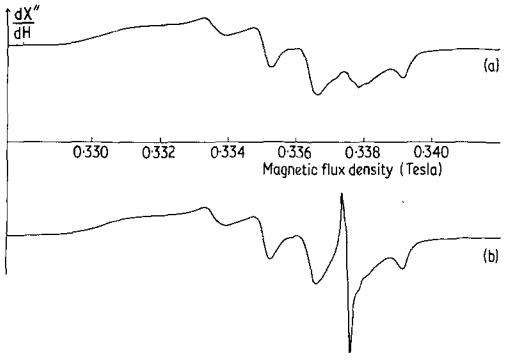

Figure 1 (a) The BOHC spectrum. Microwave power 40 mW. (b) The BOHC and trapped electron spectrum. Microwave power 0.05 mW. Dose 8598 Mrad.

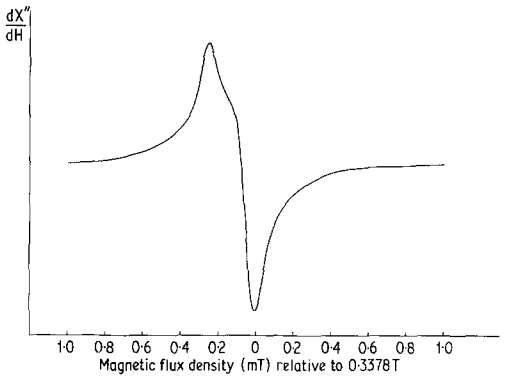

Figure 2 The trapped-electron signal obtained by subtraction of Fig. 1a from Fig. 1b. The lineshape is dose-independent.

electrons generating the narrow signal. Curves (a) and (b) of Fig. 1 can be algebraically subtracted to yield the spectrum of the trapped electrons alone. This is shown in Fig. 2 on an enlarged scale.

3.2. Growth curves

Curves such as Fig. 1a and Fig. 2 are numerically integrated twice, together with that of the copper sulphate standard, in order to determine the absolute numbers of centres contributing to the background BOHC resonance and to the electron resonance. The whole process repeated at different total doses gives the growth curves of Fig. 3. The growth of the BOHC resonance is similar to that observed in Corning 7740 Pyrex by diSalvo *et al.* [6] and agrees with the theories of Levy [7] and Cropper [8]. The behaviour of the Fe^{3+} resonance at $g = 4.29$ in γ-irradiated Pyrex has been studied in detail [2] and the relevant growth curve is presented in Fig. 4.

4. Discussion

Before attempting to correlate the growth behaviour of electron and hole centres, it is useful to describe briefly the possible nature of the trap

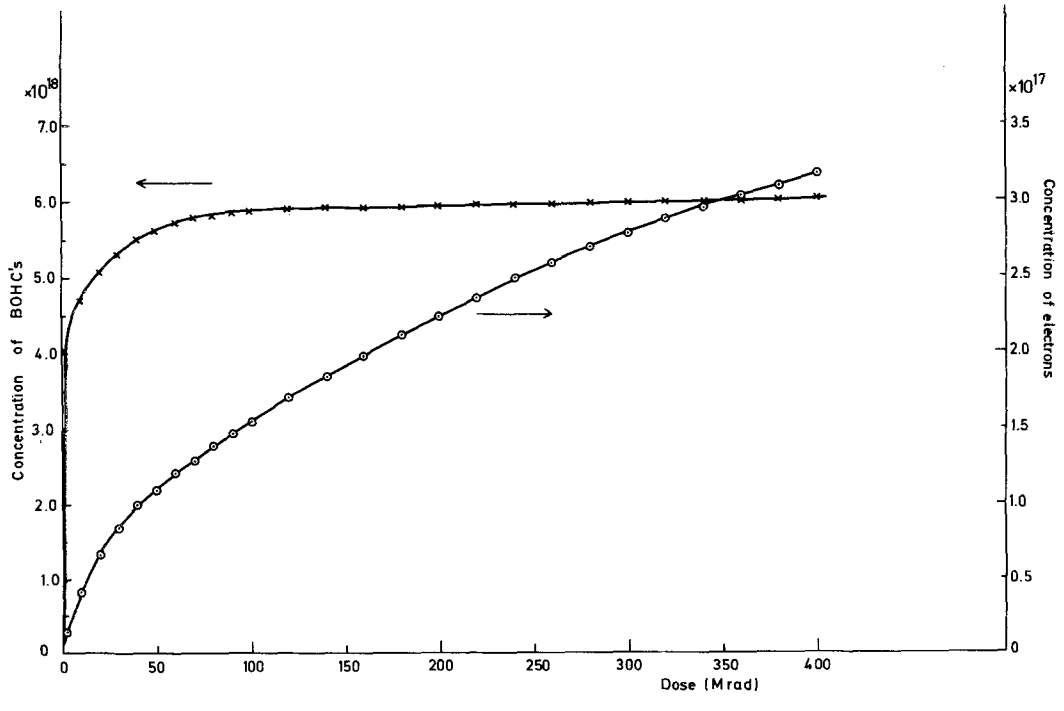

Figure 3 Growth curves of the BOHC and trapped-electron centre. Microwave power 0.05 mW, sample volume 1.66 cm^3.

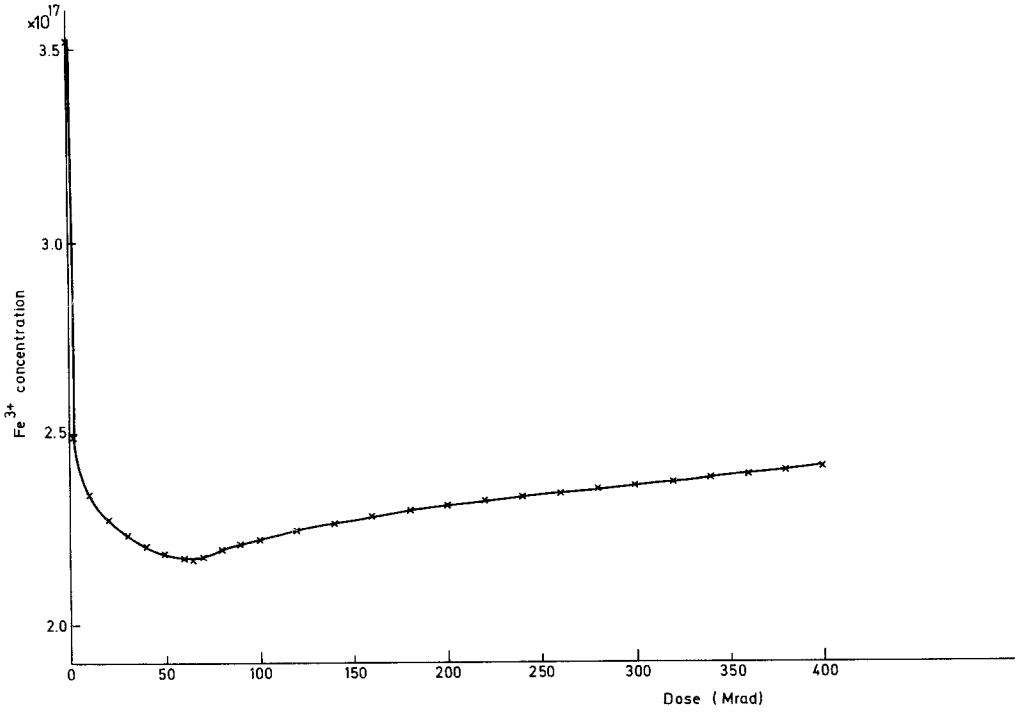

Figure 4 Variation of Fe^{3+} concentration with γ dose. Microwave power 10 mW, sample volume 1.66 cm^3.

which generates the narrow component of Fig. 1b, and to summarize the evidence for it being an electron trap.

4.1. The nature of the electron trap

Lee and Bray [3] first observed a single, sharp line superimposed on the BOHC resonance in γ-irradiated Corning 7740 Pyrex. The g-value was 2.0012 and the line was attributed to trapped electrons because of its similarity to the trapped-electron resonance found in irradiated silica glass by Weeks [9]. This trap was originally thought to be an oxygen vacancy [10], although later work indicated that the electron was trapped on a silicon atom [11].

A different type of trap for electrons was discovered originally in liquid ammonia [12] and subsequently in organic glasses [13] and in polymers [14]. In each case a narrow singlet is obtained, and it is attributed to electrons trapped in pre-existing voids of molecular dimensions. In the earlier stages of the present work, when the Fe^{3+} resonance was being investigated [2], it was suggested by the author that the principal electron trap in Pyrex was a void in the glass. More recent work has provided evidence to the contrary. It is not the purpose of the present paper to derive a detailed model for this electron trap, but the reasoning which reduced the credibility of the void trap has given further insight into the borosilicate structure, hence this small digression.

4.1.1. Electron resonances in silicate and borosilicate glasses

The narrow resonance observed in γ-irradiated Corning 7740 Pyrex by Lee and Bray [3] was a singlet of g-value 2.0012 ± 0.0008. The electron resonance observed by Weeks [9] in irradiated silica glass had a complex shape, being the envelope of the spectrum observed in single-crystal quartz averaged over all orientations, with a g-value of 2.0013 ± 0.0004. From the similarities of the shapes, widths and g-values, the narrow resonance in Pyrex was also attributed to a trapped electron.

Some high-purity silica glass has been γ-irradiated under the same conditions as the Pyrex, and the spectrum obtained is shown in Fig. 5. The similarity between this and the spectrum of Fig. 2 is obvious if some line broadening is taken into account. Sodium bisilicate glass, $Na_2O \cdot 2SiO_2$, also reveals this characteristic shape [15], but the intensity is very much reduced. In order to accentuate the very close similarity of these resonances, second-derivative spectra were recorded. The spectrum from the Pyrex glass is shown in Fig. 6, resolving two peaks, A and B. Table I compares the

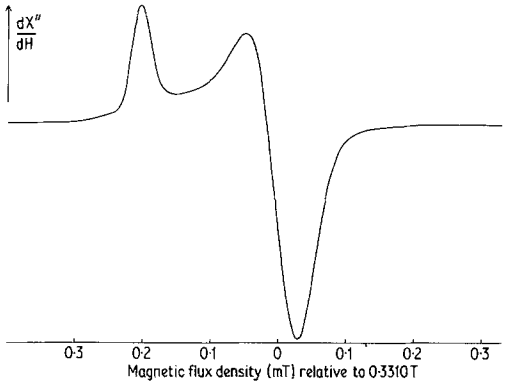

Figure 5 Characteristic spectrum of γ-irradiated silica glass. Microwave power 0.2 mW.

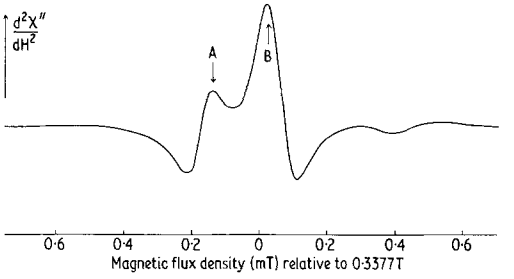

Figure 6 Second derivative spectrum of the electron centre in Pyrex. Microwave power 0.05 mW.

TABLE I A comparison of the g-values at the second-derivative maxima (see Fig. 6) in three different glasses. The relative accuracy of these figures is ± 0.0001, the absolute accuracy ± 0.0004.

	Silica glass	Pyrex glass	Bisilicate glass
g_A	2.0020	2.0018	2.0018
g_B	2.0009	2.0008	2.0009

g-values at the peaks for silica glass, Pyrex and sodium bisilicate glass. These figures indicate quite clearly that the electron trapping centre is the same in each glass. (The discrepancy between the value of g_B for silica (2.0009) in Table I and that determined by Weeks (2.0013) can be explained quite simply. Week's measurement of g-values gave $g = 2.0041$ for DPPH [9]; the present measurements use $g = 2.0036$ for DPPH as their reference. If Week's value of $g = 2.0013$ is corrected to the 2.0036 DPPH standard, the result obtained is $g = 2.0008$, in close agreement with the present figure.)

The figures of Table I, showing the existence of a common electron trap, immediately suggest that there should be a constituent common to these glasses. Silica is the only constituent to fit this description and, because borate glasses do not form this particular electron trap [3], the Pyrex electron trap is considerably simpler than it otherwise might have been. However, the correlation of the traps with the presence of silica in the melt is only the beginning of the story. Pyrex glass and sodium bisilicate glass have roughly the same molecular concentration of silica, yet the numbers of electrons that they trap for a given γ dose are orders of magnitude different [15]. In silicate structures, a silicon atom is always linked to four oxygen atoms [16] so again, the numbers of SiO_4 tetrahedra in the two types of glass should be very similar. A possible clue towards solving this paradox is provided in the work of Weeks and Nelson [10] in their analysis of the electron centre in silica glass and in crystalline quartz. The centre in a quartz crystal was labelled E_1' by them for ease of reference. Using the eigenvalues of the g tensor of the E_1' centre, they derived the envelope of the resonance found in silica glass to such an accuracy that the postulate of randomly oriented SiO_4 tetrahedra was questioned. In other words, a short-range correlation of the tetrahedra (probably between 5 and 10 Å) was suggested, similar to the α phase in crystalline quartz. It is well known that most glasses possess sub-microscopic crystalline structure [17], this structure having been revealed by optical scattering [18], neutron diffraction [19], density measurements [20] and electron microscopy [21]. In rather complex borosilicates [21], helical structures 30 Å wide and several hundred Å long have been observed, while other such glasses contained even longer silica chains.

With this structural evidence, the following conclusions may be reached:

(a) The SiO_4 tetrahedra existing as an integral part of the borosilicate or bisilicate structure do not contribute to the narrow electron line under investigation.

(b) Existing as *sub-microscopic* structure are helices or chains of silica. Averaged over the volume of the glass, this substructure is basically random, but over distances up to about 10 Å there is some correlation between adjacent SiO_4 tetrahedra.

(c) It is the substructure (sub-microscopic threads of silica glass) which forms the same electron trap as in bulk silica glass, and the presence of short-range order is revealed by the characteristic lineshape (Fig. 2 in the case of Pyrex, Fig. 5 in the case of silica) which can be derived from the eigenvalues of the g tensor of single-crystal silica.

(d) Because the bisilicate glass traps considerably fewer electrons than Pyrex does, the amount of

silica substructure in the bisilicate must be very much less.

Having proposed this general model for the electron trap which generates the narrow component in the irradiated Pyrex esr spectrum, the discussion can revert to the growth behaviour of the electron and hole centres.

4.2. Growth of the electron and hole centres

The growth curves of Figs. 3 and 4 can be linearized by adopting a logarithmic dose axis, as shown in Figs. 7 and 8. The derivation of the dotted and broken lines in Fig. 8 is discussed fully in [2]. From these characteristics, one feature is common:

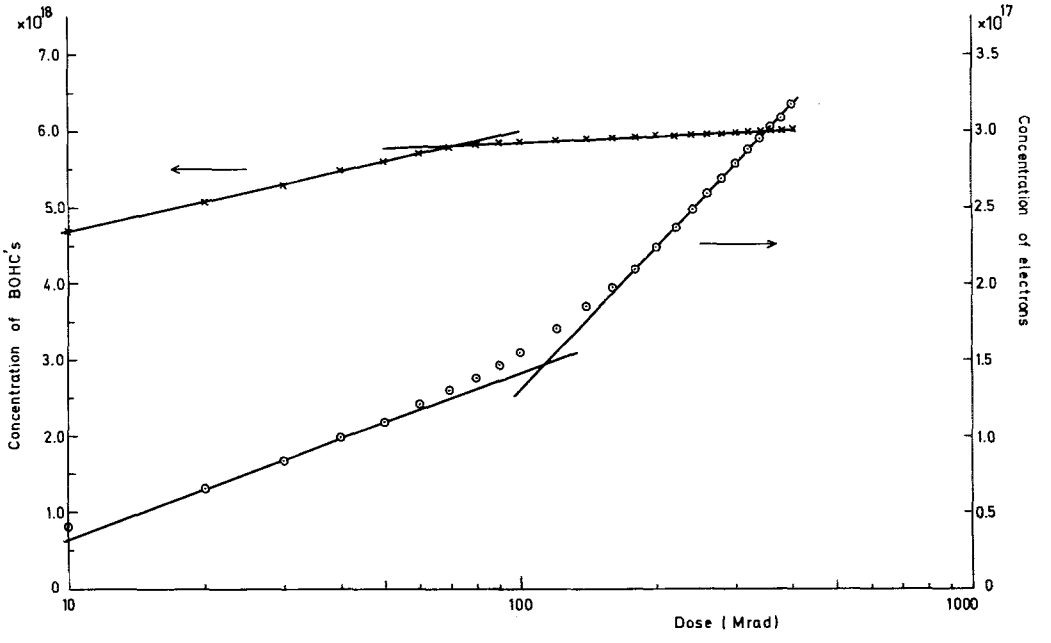

Figure 7 Variations of the BOHC and trapped-electron populations as functions of γ dose. Microwave power 0.05 mW, sample volume 1.66 cm^3.

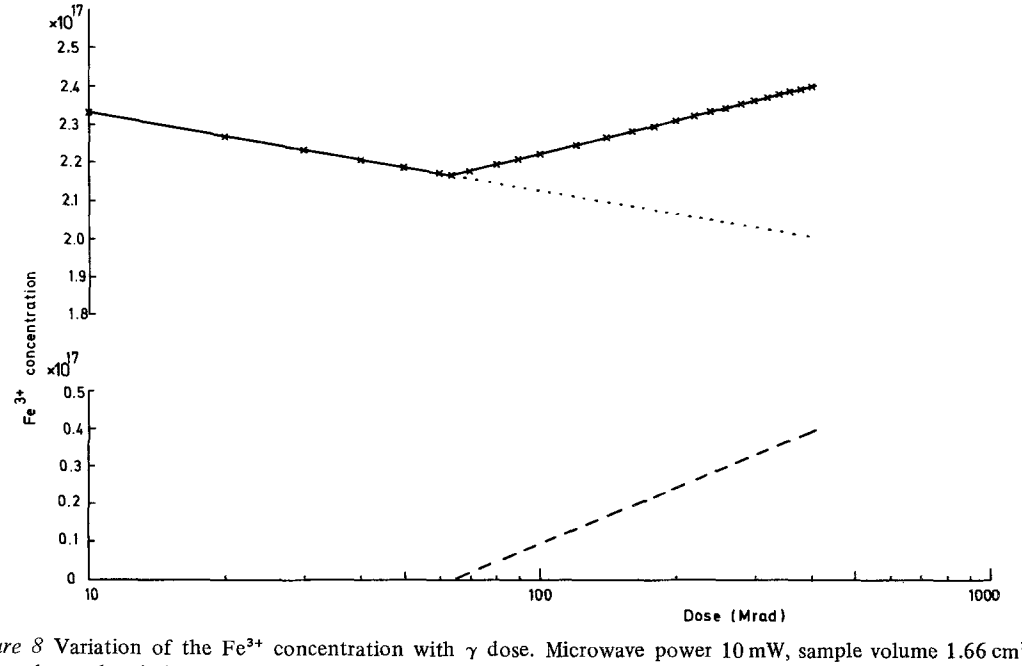

Figure 8 Variation of the Fe^{3+} concentration with γ dose. Microwave power 10 mW, sample volume 1.66 cm^3. Full line – observed variation. Dotted line – extrapolated reduction process. Broken line – derived oxidation process.

each type of centre has a growth behaviour which is divisible into two regions, low-dose and high-dose. The two regions have a common diffuse boundary centred at about 100 Mrad. The detailed behaviour of the BOHC growth and the Fe^{3+} growth has already been described [2], but will be outlined here in order to present a complete picture of the trapping mechanisms.

4.2.1. The low-dose region

The principal hole trap is an oxygen atom bridging two boron atoms [4]. On trapping a hole, it forms the boron–oxygen hole centre (BOHC). The second hole trap is Fe^{2+} [22, 23], which forms Fe^{3+} after trapping a hole. The two electron traps are the silica substructure (described in Section 4.1.1), and the Fe^{3+} ion [22] which produces Fe^{2+} after trapping an electron. Ferrous and ferric iron are known to coexist in glasses [24–27] irrespective of the valence state present in the components of the melt. In the Pyrex samples used, iron exists as an impurity at a chemically determined level of 0.027 wt%.

As irradiation proceeds, the electrons and holes so formed proceed to their respective traps. From evidence previously presented [2], the holes are known to be trapped entirely on boron-associated oxygen atoms, to the exclusion of the Fe^{2+} hole traps. Electrons divide between silica-type traps and Fe^{3+} traps, the latter forming Fe^{2+} which cannot be observed by esr at room temperature [28]. These three processes cause the growth of the BOHC signal, the growth of the silica-type signal (Fig. 3), and the diminution of the Fe^{3+} signal (Fig. 4).

4.2.2. The high-dose region

At a total dose of about 65 Mrad, Fig. 3 shows that the dominant hole traps are 96% full. At this point, the migrant holes become aware of the Fe^{2+} ions as alternative traps and begin to fill them. This produces Fe^{3+}, a process in opposition to the continuing electron capture by Fe^{3+}, producing Fe^{2+}. It can be seen from Fig. 4 that more Fe^{3+} is being generated from hole capture by Fe^{2+} than is being lost through electron capture by Fe^{3+} itself. Fig. 8 shows the electron-capture process extrapolated into the high-dose region and the hole-capture process by Fe^{2+} which begins in the high-dose region.

An examination of Fig. 7 shows that the electron trapping which occurs in the silica substructure undergoes a gradual, positive, rate change during the transition from the low-dose to the high-dose region. The most likely cause of this is the behaviour of the other electron trap, Fe^{3+}. At about 65 Mrad, the depletion of the original Fe^{3+} population is beginning to saturate and, as a result, the electrons become trapped at silica-type sites at a greater rate than before, causing the behaviour shown in Fig. 7.

4.3. Analysis

It is not within the scope of the present work to enter into a detailed analysis of the kinetics of growth of the various centres considered so far. A purely empirical approach is adopted, to illustrate most clearly the significances of the characteristics shown in the diagrams.

4.3.1. The high-dose region

Consider Figs. 7 and 8. Using concentration units of 10^{17} and Mrad dose units, the equations for the growth lines can be derived.

(a) For BOHC's, the concentration N_B at a dose D is given by

$$N_B = 1.1 \log_e D + 53.4. \quad (1)$$

(b) For holes trapped by Fe^{2+},

$$N_H = 0.21 \log_e D - 0.86. \quad (2)$$

(c) For electrons trapped by Fe^{3+},

$$N_E = 0.09 \log_e D + 0.99. \quad (3)$$

(d) For electrons trapped in the silica substructure,

$$T_E = 1.35 \log_e D - 4.91. \quad (4)$$

If these four mechanisms are accurate in accounting for the trapping, the numbers of electrons and holes trapped, over the same dosage increment, should balance. In other words, does the equation

$$N_B + N_H = T_E + N_E \quad (5)$$

hold in the high-dose region? This is most easily checked by equating the "rate" constants:

$$\underset{\text{Boron}}{1.1} + \underset{Fe^{2+}}{0.21} \simeq \underset{\text{Silica}}{1.35} + \underset{Fe^{3+}}{0.09}. \quad (6)$$

There is equality here, to within experimental error; each number is identified by the type of trap written below it. Equation 6 has more immediate meaning if it is scaled up to indicate how 100 electron-hole pairs would distribute themselves:

$$\underset{\text{Boron}}{80} + \underset{\text{Holes}}{\underset{\text{Fe}^{2+}}{15}} \simeq \underset{\text{Silica}}{98} + \underset{\text{Electrons}}{\underset{\text{Fe}^{3+}}{7}} . \quad (7)$$

The equation is obviously accurate to 5%, and shows that the assumption of four traps is correct.

4.3.2. The low-dose region

Again, working in concentration units of 10^{17} and Mrad dose units, the corresponding equations become:

(a) for BOHC's,

$$N_B = 5.6 \log_e D + 34.1; \quad (8)$$

(b) there are no holes trapped by Fe^{2+} in the low-dose region [2];

(c) for electrons trapped by Fe^{3+},

$$N_E = 0.09 \log_e D + 0.99; \quad (9)$$

(d) for electrons trapped in the silica substructure,

$$T_E = 0.48 \log_e D - 0.79. \quad (10)$$

It is immediately obvious that the rate constants of these equations are *not* going to balance, the implication being that there must be an electron trap (or traps) unaccounted for. This is not at all surprising because esr detects only those traps characterized by an unpaired spin. If a capture centre is of the spin-paired type, it is undetectable by esr.

In view of this, suppose that there is such an electron trap. The rate constants of Equations 8 to 10 can now be made to balance:

$$\underset{\text{Boron}}{5.6} = \underset{\text{Fe}^{3+}}{0.09} + \underset{\text{Silica}}{0.48} + \underset{\text{Unknown}}{5.03} . \quad (11)$$

Or, in terms of 100 electron-hole pairs:

$$\underset{\text{Boron}}{100} = \underset{\text{Fe}^{3+}}{2} + \underset{\text{Silica}}{9} + \underset{\text{Unknown}}{89} . \quad (12)$$

(In evaluating Equations 7 and 12, the nearest integer is quoted in cases where interpolation yields fractions of an electron or hole.) This provides quite strong, indirect, evidence for the existence of a major electron trap which is undetectable by electron spin resonance at room temperature.

Griscom [29], in a low-temperature study of X-irradiated alkali borate glasses, postulated the existence of an intrinsic defect, the boron electron centre (BEC). This centre, which is readily destroyed by visible light or by thermal annealing above 100 K, accounts for only about 15% of the total number of trapped electrons needed to balance the trapped hole population at 77 K. Direct evidence is then given [30] that the remaining 85% become trapped on alkali ions, or complexes thereof. Having trapped their electrons, the alkali ions tend to cluster. As the temperature rises, clustering proceeds more rapidly, producing major agglomerations. This is the reason for the spectrum disappearing at room temperature — the clusters form large complexes in which the electrons are spin-paired. It is possible, therefore, that the unknown centre introduced into Equations 11 and 12 is the alkali-associated centre. Because the irradiation takes place at room temperature, formation and clustering into a non-paramagnetic form will occur quickly. The BEC will never exist at room temperature, so it would seem reasonable that Equation 12 is a true representation of the trapping process in γ-irradiated Pyrex in the low-dose region at room temperature. The accuracy of Equation 7 in describing the high-dose situation would suggest that the electron trapping of the alkali-associated centres has reached full saturation. This is to be expected, since clustering cannot proceed indefinitely.

5. Conclusions

Electron spin resonance has been used to investigate γ-irradiated Pyrex glass. A very narrow resonance has been found at $g = 2.0008$, in agreement with earlier work [3]. The lineshape has been compared with similar resonances in silica glass and in sodium bisilicate glass, and very strong evidence has been found that the electron trapping centre is the same in all cases. It is then argued that the electron trap is *not* part of the bulk bisilicate or borosilicate structure, but instead is part of a sub-microscopic silica structure possessing the same short range order that exists in silica glass.

A detailed consideration of the growth curves of the various electron and hole traps with γ dose has again revealed the two-region process reported recently [2]. In the high-dose region, the growths of the electron and hole populations are shown to balance quite accurately. In the low-dose region, however, a large imbalance of the populations has led to the proposal of a non-paramagnetic trapped-electron population. It is quite possible that the basic trap is the alkali-associated centre postulated by Griscom [30]. At room temperature, these

alkali ions with their trapped electrons will cluster into large complexes which are spin-paired and hence non-paramagnetic. Future work on this subject will include a low-temperature investigation in an attempt to reveal the alkali-associated centre in Pyrex and to verify the proposed model of trapping in the low-dose region.

References

1. E. L. YASAITIS and B. SMALLER, *Phys. Rev.* **92** (1953) 1068.
2. G. BROWN, *J. Mater. Sci.* **10** (1975) 1481.
3. S. LEE and P. J. BRAY, *J. Chem. Phys.* **39** (1963) 2863.
4. D. L. GRISCOM, P. C. TAYLOR, D. A. WARE and P. J. BRAY, *ibid* **48** (1968) 5158.
5. P. C. TAYLOR and D. L. GRISCOM, *ibid* **55** (1971) 3610.
6. R. DI SALVO, D. M. ROY and L. N. MULAY, *J. Amer. Ceram. Soc.* **55** (1972) 536.
7. P. W. LEVY, *ibid* **43** (1960) 389.
8. W. H. CROPPER, *ibid* **45** (1962) 293.
9. R. A. WEEKS, *J. Appl. Phys.* **27** (1956) 1376.
10. R. A. WEEKS and C. M. NELSON, *ibid* **31** (1960) 1555.
11. R. H. SILSBEE, *ibid*, **32** (1961) 1459.
12. J. JORTNER, *J. Chem. Phys.* **30** (1959) 839.
13. A. EKSTROM and J. E. WILLARD, *J. Phys. Chem.* **72** (1968) 4599.
14. R. M. KEYSER, K. TSUJI and F. WILLIAMS, "The Radiation Chemistry of Macromolecules", Vol. 1 (Academic Press, New York, 1972).
15. G. BROWN, unpublished work.
16. H. LIPSON and W. COCHRAN, "The Determination of Crystal Structures" (Bell, London, 1957).
17. K. H. SUN and N. J. KREIDL, *Glass Ind.* **33** (1952) 589.
18. P. DEBYE and A. M. BUECHE, *J. Appl. Phys.* **20** (1949) 518.
19. W. O. MILLIGAN, H. A. LEVY and S. W. PETERSON, *Phys. Rev.* **83** (1951) 226.
20. R. W. DOUGLAS, *Glass Ind.* **32** (1951) 238.
21. A. F. PREBUS and J. W. MICHENER, *Bull. Amer. Phys. Soc.* **27** (1952) 25.
22. R. F. TUCKER, "Advances in Glass Technology" (Plenum Press, New York, 1962).
23. J. S. STROUD, J. W. H. SCHREURS and R. F. TUCKER, "Proceedings of the 7th International Glass Congress, Brussels 1965" (Gordon and Breach, New York, 1966).
24. A. A. BELYUSTIN, YU. M. OSTANEVICH, A. M. PISAREVSKII, S. B. TOMILOV, U. BAI-SHI and L. CHER, *Sov. Phys. Sol. Stat.* **7** (1965) 1163.
25. J. P. GOSSELIN, U. SHIMONY, L. GRODZINS and A. R. COOPER, *Phys. Chem. Glasses* **8** (1967) 56.
26. A. M. BISHAY and L. MAKAR, *J. Amer. Ceram. Soc.* **52** (1969) 605.
27. M. F. TARAGIN and J. C. EISENSTEIN, *J. Non-Cryst. Solids* **3** (1970) 311.
28. B. BLEANEY and K. W. H. STEVENS, *Rep. Progr. Phys.* **16** (1953) 108.
29. D. L. GRISCOM, *J. Chem. Phys.* **55** (1971) 1113.
30. *Idem, J. Non-Cryst. Solids* **6** (1971) 275.

Received 21 April and accepted 20 May 1975.